Electric-Field-Induced Magnetic Anisotropy in a Nanomagnet Investigated on the Atomic Scale

A. Sonntag,* J. Hermenau, A. Schlenhoff, J. Friedlein, S. Krause, and R. Wiesendanger
Institute of Applied Physics and Interdisciplinary Nanoscience Center Hamburg, University of Hamburg, Jungiusstrasse 11, 20355 Hamburg, Germany
(Received 28 August 2013; published 8 January 2014)

Magnetoelectric coupling is studied using the electric field between the tip of a spin-polarized scanning tunneling microscope and a nanomagnet. Our experiments show that a negative (positive) electric field stabilizes (destabilizes) in-plane magnetization against thermal agitation, whereas it destabilizes (stabilizes) out-of-plane magnetization. We conclude that the electric field E induces a uniaxial anisotropy that favors in-plane magnetization for $E < 0$ and out-of-plane magnetization for $E > 0$. Our experiments demonstrate magnetic manipulation on the atomic scale without exploiting spin or charge currents.

DOI: 10.1103/PhysRevLett.112.017204 PACS numbers: 75.85.+t, 68.37.Ef, 75.30.Gw, 75.70.Ak

Manipulating magnetic properties with an electric field is in the focus of ongoing extensive research in the field of spintronics [1–9]. Especially, tuning the magnetic anisotropy by an electric field is a promising candidate for solving the fundamental dilemma in data storage applications: Whereas a large anisotropy is needed to stabilize a magnetic bit against thermal agitation, a low anisotropy is desired during magnetization reversal when writing information. An electric field can maximize or momentarily decrease the magnetic anisotropy [10–12], thereby stabilizing a magnetic bit for long-term storage or facilitating magnetization reversal when writing information. As virtually no current is needed for this electric-field-based scheme, such devices could benefit from smaller power consumption compared to conventional magnetic field or spin-transfer torque based devices.

Experiments on semiconductors [1,2,5], multiferroic materials [3,6] or metals [4,7,13,14] demonstrated that an electric field can modify the magnetic properties via magnetoelectric coupling. Here, metallic systems have received considerable attention due to the potential easy integration into spintronic devices. However, in metals the electric field is screened by free electrons and, thus, cannot penetrate the bulk. Therefore, electric-field-induced modifications of the magnetic properties can only be expected at the surface and in thin-film systems. To our knowledge all studies to date were performed on layered extended thin films where the electric field is applied across an insulating layer of electrolyte or dielectric material [4,7,13,14]. The preparation of these systems is challenging, since imperfections like local inhomogeneities and defects can complicate the correct interpretation of the experiments. In our studies using spin-polarized scanning tunneling microscopy (SP-STM), we realize a well-defined, atomically sharp magnet-to-vacuum interface and address single, defect-free magnets on the atomic scale for electric-field-induced manipulation of their magnetic properties.

Figure 1(a) illustrates our experimental approach: A ferromagnetic nanoisland consisting of only a few atoms is placed on a metallic substrate, and an electric field is applied by approaching a biased scanning probe tip. In this setup, the magnetoelectric coupling is maximized by reducing the thickness of the nanomagnet to a single atomic layer.

Our experiments were performed under ultrahigh vacuum conditions with a pressure below 1×10^{-8} Pa using a home-built variable temperature SP-STM. In the microscope, both the tip and the sample are cooled by a

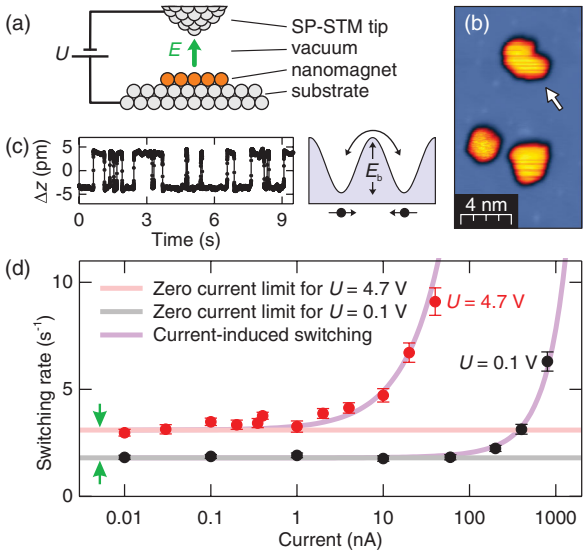

FIG. 1. (a) Scheme of the experimental setup. (b) Spin-polarized STM topography taken at $U = -100$ mV, $I = 2$ nA, $T = 45$ K. (c) Telegraph signal observed when the tip is positioned above the island marked in (b) and scheme for thermal magnetization reversal. (d) Switching rate of the island as a function of tunnel current for two different bias voltages (lines are guides to the eye).

continuous flow He cryostat. Tungsten and molybdenum substrates were prepared by annealing in oxygen atmosphere and subsequent high temperature flashes [15].

Depositing iron onto these substrates leads to the pseudomorphic formation of atomic-scale monolayer nanoislands that are found to be ferromagnetic at cryogenic temperatures. When prepared on W(110) they exhibit an in-plane uniaxial magnetic anisotropy with the easy axis of magnetization lying in the $[1\bar{1}0]$ direction [16,17]. In contrast, when prepared on Mo(110), the easy axis is pointing out of the surface plane [18].

Figure 1(b) shows an SP-STM topography map of three Fe nanomagnets on a W(110) substrate, taken with an in-plane sensitive bulk Cr tip. The nanomagnets consist of about 100 to 150 atoms and frequently switch their magnetic orientation due to thermal agitation at the given temperature of 45 K. In SP-STM, the tunnel current I is proportional to the projection of the magnetization of the tip onto the magnetization of the sample. As the measurements are performed in constant current mode, the distance between tip and sample z has to be adjusted whenever the nanomagnet reverses its magnetization. Therefore, a telegraphic noise pattern emerges in z, as can be seen in Fig. 1(c). Consequently, the magnetic orientation of the nanomagnet can be recorded in real time, and the switching rate ν can be derived.

As has been shown before, ν can be described by a Néel-Brown law [18–22]

$$\nu = \nu_0 \exp\left(-\frac{E_b}{k_B T}\right). \quad (1)$$

Here, $k_B T$ is the thermal energy, E_b the energy barrier that has to be overcome during magnetization reversal and ν_0 the attempt frequency.

The switching rate of an individual island was analyzed as a function of tunnel current I for two different bias voltages U, as can be seen in Fig. 1(d). More than 1000 switching events were recorded and evaluated for every data point. In agreement with previous studies, Joule heating strongly increases the switching rate when large currents are applied [23–25]. For low currents of $I \leq 1$ nA we observe a constant switching rate as Joule heating is negligible in this regime. Although we expect to find the intrinsic switching rate for a vanishing tunnel current, irrespective of the bias voltage, the zero current limit of the switching rate at $U = 0.1$ V clearly deviates from that at $U = 4.7$ V. This indicates that an additional, current independent effect modifies the switching behavior of the nanomagnet.

In Fig. 2(a), the telegraphic noise on another Fe/W(110) nanomagnet is shown for three different bias voltages at a very low tunnel current of 100 pA. Compared to the time trace recorded at 50 mV, the switching rate is again increased for a high positive bias voltage. Surprisingly,

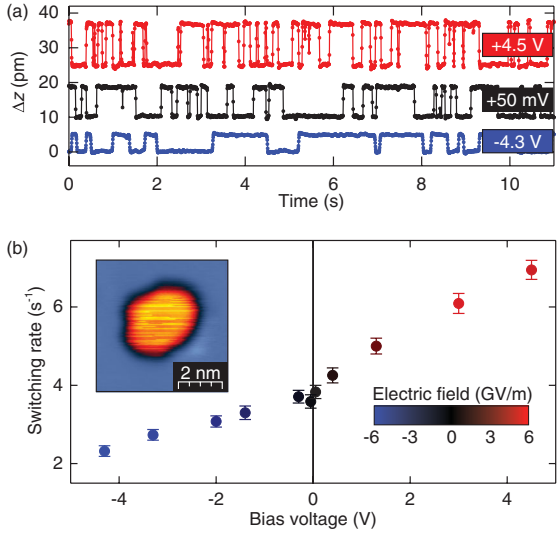

FIG. 2. (a) Time traces recorded at different bias voltages. Curves were offset for clarity. (b) Switching rate as a function of applied bias voltage. Data points are color coded with the electric field between tip and sample. All measurements were performed at $I = 100$ pA, $T = 45$ K. The inset shows the topography of the investigated island.

the switching rate seems to be decreased when a high negative bias voltage is applied. The switching rate as a function of bias voltage is shown in Fig. 2(b). A clear trend from low switching rate at negative bias to high switching rate at positive bias is visible, ν being tunable by a factor of almost 4 between -5 and $+5$ V. The effect is volatile meaning that as soon as the bias voltage is reduced to almost zero, the switching rate of the island takes the intrinsic value.

The question arises how a change of the bias voltage can induce a change in the switching behavior of the nanomagnet. When changing U the tip-to-sample distance has to be adjusted in order to keep the tunnel current constant. However, when changing the bias voltage by 2 orders of magnitude, the distance is only varied by a factor of 3 [26]. Consequently, the electric field increases significantly with increasing bias voltage. Therefore, we attribute the observed modification of ν with U to the coupling of the nanomagnet to the electric field E. Values of E are derived from $z(U)$ measurements [26], resulting in a maximum of $E \approx \pm 6$ GV/m at $U = \pm 5$ V. The electric field is used as a color coding in Fig. 2(b), indicating the direct relation between switching rate and the electric field strength.

In a simple picture, the electric field causes a charge redistribution at the surface of the nanomagnet. Positive fields lead to a depletion and negative fields to an accumulation of electrons. This in turn leads to a shift of the Fermi level and a modification of the occupation of the $3d$ bands which are responsible for magnetism [7]. Recently, a generalized perturbation approach showed that a positive

electric field can induce out-of-plane magnetic anisotropy due to Rashba spin-orbit coupling [27]. A more detailed understanding of the coupling mechanism can be achieved by first principle calculations. These have been performed, for example, on free standing Fe films [10] or Fe/MgO and MgO/Fe/MgO structures [28], revealing that the strength, sign and polarity symmetry of the effect can vary strongly from system to system.

In our experiment, the electric field obviously modifies the energy barrier that has to be overcome during magnetization reversal. For $E < 0$ the switching rate is decreased, indicating an increase of the energy barrier [see Eq. (1)]. Likewise, the switching rate is increased for $E > 0$, corresponding to a decrease of E_b. We attribute the change of E_b to magnetic anisotropy induced by the electric field. In a simple model, it superimposes the intrinsic anisotropy, as illustrated in Fig. 3(a). For $E < 0$, the magnetoelectric coupling favors in-plane magnetization, whereas for $E > 0$, an out-of-plane magnetization is preferred. This results in a stabilization or destabilization of the in-plane Fe/W(110) nanomagnet against thermal agitation, respectively.

Depositing the same iron nanomagnets onto a Mo(110) substrate results in a system with an easy axis of magnetization pointing out of the surface plane [18]. Since the lattice constant, chemical properties, and, thus, the electronic structure of molybdenum are similar compared to tungsten, it is reasonable to assume that the mechanism of magnetoelectric coupling is the same on Fe/W(110) and Fe/Mo(110). However, an inversion of the electric-field-induced modification of the switching behavior is expected when changing between the two systems: the out-of-plane system is destabilized for $E < 0$ and stabilized for $E > 0$, as illustrated in Fig. 3(b).

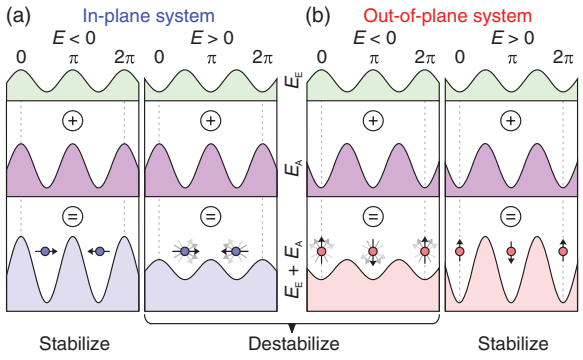

FIG. 3. Schematics of the anisotropy energy as a function of the polar angle θ of a magnetic system under the influence of an electric field. The top row shows the energy contribution from the electric field E_E, the second row the undisturbed system E_A, and the third row the effective energy given by the sum of E_E and E_A. The electric field either favors in-plane ($E < 0$) or out-of-plane ($E > 0$) orientation of the magnetization. While the coupling mechanism is exactly the same for the in-plane system (a) and the out-of-plane system (b), the impact on the switching behavior is reversed: e.g., for $E < 0$ the in-plane system is stabilized, whereas the out-of-plane system is destabilized.

Results of SP-STM experiments to validate this phenomenological model are shown in Fig. 4. The same tip could be used for the out-of-plane system since bulk Cr tips are known to be sensitive to both in-plane and out-of-plane magnetization [29]. The inset in Fig. 4 shows the topography of a Fe/Mo(110) nanomagnet that reverses its magnetization at an intrinsic switching rate of 8 s^{-1} due to thermal agitation. As in the case of the in-plane system, we measured the switching rate as a function of U at low I. The switching rate could be adjusted to be between 3 and 17 s^{-1} by changing the bias voltage. We find a higher switching rate for $E < 0$ and a lower rate for $E > 0$. This is in contrast to the results on the in-plane Fe/W(110) nanomagnets and, thereby, in perfect agreement with our expectations. Hence, we conclude that the coupling mechanism is analogous in this system and that the electric field indeed induces an additional magnetic anisotropy in the nanomagnet.

To quantify the strength of the magnetoelectric coupling we modify the energy barrier with an E-field dependent contribution: $E_b \rightarrow E_b + \Delta E_b(E)$. The energy barrier variation $\Delta E_b(E)$ can then be calculated from Eq. (1):

$$\Delta E_b(E) = k_B T \ln\left(\frac{\nu_{int}}{\nu(E)}\right), \quad (2)$$

where ν_{int} is the intrinsic switching rate at vanishing bias voltage.

A comparison of ΔE_b on Fe/W(110) and Fe/Mo(110) is shown in Fig. 5. We find energy barrier variations of up to $\Delta E_b = \pm 2$ meV. This is a small change, compared to the intrinsic energy barrier of $E_b = 60$ meV for Fe/Mo(110) and $E_b = 125$ meV for Fe/W(110). Nevertheless, the electric field significantly alters the switching behavior, as ν depends exponentially on ΔE_b. The strength of the effect is comparable to spin transfer

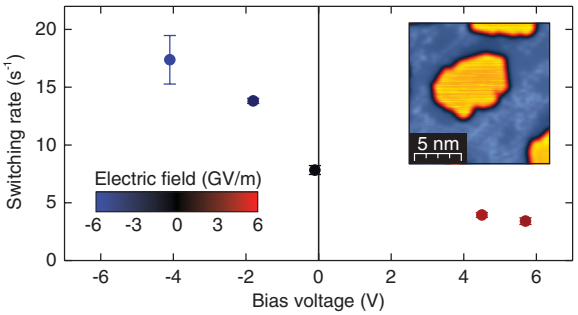

FIG. 4. Switching rate as a function of applied bias voltage for the Fe/Mo(110) nanomagnet. Data points are color coded with the electric field strength. $I = 100$ pA, $T = 26.5$ K. The inset shows the topography of the island.

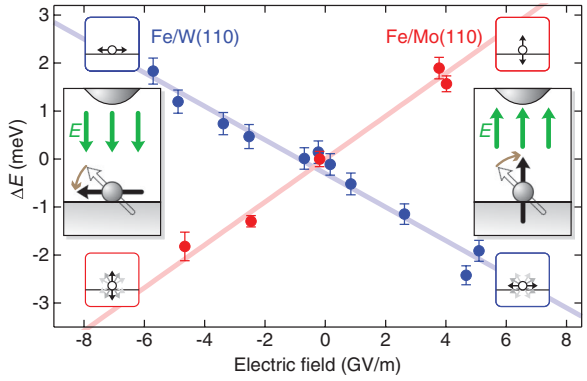

FIG. 5. Electric-field-dependent energy barrier variation for the in-plane system Fe/W(110) and the out-of-plane system Fe/Mo(110). Negative electric fields favor in-plane, positive electric fields out-of-plane orientation of the magnetization.

torque (STT) at elevated tunneling currents observed on the same sample system ($\Delta E_{\mathrm{b,STT}} = 1.5$ meV at 1000 nA) [24,25]. Note that the STT generates a directed switching but does not change the magnetic anisotropy.

The out-of-plane Fe/Mo(110) islands switch their magnetization via a coherent rotation [18]. In this case $E_{\mathrm{b}} = KV$ with the magnetic anisotropy K and the volume of the island V. We can calculate the change of the magnetic anisotropy $\Delta K(E)$ as a function of electric field

$$\Delta K(E) = \Delta E_{\mathrm{b}}(E)/V. \tag{3}$$

Using this relation, we find that the variation of anisotropy mounts up to 68 kJ/m^3. The intrinsic anisotropy was determined to be $K = 1100$ kJ/m^3 [18]. Consequently, the anisotropy can be changed by 6% in our experiments. Conventionally, the anisotropy variation is attributed to a change of the surface anisotropy ΔK_{s}, resulting in a change of 14 μJ/m^2.

To compare this value with studies on different systems, we refer to an electric field of 1 GV/m. For this field, we obtain $\Delta K_{\mathrm{s}} = 1.6$ μJ/m^2. Significantly higher values ranging from 33 up to 93 μJ/m^2 have been reported in the literature [7,13,14]. However, all of these experiments rely on the use of a dielectric material as an insulating barrier between the electrode and the magnetic film. This significantly increases the charge accumulation at the surface of the magnetic film compared to the case of a vacuum barrier [11]. Since the electron accumulation is the origin of the anisotropy change, this explains the lower change of magnetic anisotropy in our experiments. To take the dielectric into account, it is reasonable to evaluate the strength of the effect in terms of a change of anisotropy per accumulated surface charge density $\sigma = \epsilon_0 \epsilon_{\mathrm{r}} E$. Here ϵ_0 is the electric constant and ϵ_{r} is the relative permittivity of the insulating layer. Referring to a surface charge density of 8.85 mC/m^2 (which is the surface charge density at 1 GV/m in the case of a vacuum barrier), the published results project to values between 3.4 and 9.5 μJ/m^2 leading to a reasonable agreement with our finding of 1.6 μJ/m^2.

Our approach to investigate magnetoelectric coupling benefits from atomically well-defined interfaces. In thin film geometry, interface roughness will create spots with a locally enhanced electric field and, thus, an inhomogeneous anisotropy. Additionally, the interface composition and intermixing will play a crucial role for magnetoelectric coupling. It has been shown, theoretically, that the magnetoelectric coupling is weak for an ideal MgO/Fe interface but can be strongly increased by the formation of an interfacial FeO layer [30]. In our experiments, an ideal, atomically sharp surface to vacuum interface is realized.

In summary, we have investigated the influence of an electric field on the magnetic properties of magnets on the atomic scale using a spin-polarized scanning tunneling microscope. Using this setup we demonstrate magnetoelectric coupling across a vacuum barrier. We find that the electric field induces a uniaxial magnetic anisotropy energy that favors in-plane magnetization for $E < 0$ and out-of-plane magnetization for $E > 0$. Consequently, negative (positive) electric fields stabilize (destabilize) in-plane magnets, whereas out-of-plane magnets are destabilized (stabilized). We have compared our results to investigations on extended thin films. Considering differences of the sample geometry, i.e., the usage of a dielectric material, we find a similar change of anisotropy in our measurements.

Our experimental technique permits us to investigate the coupling between electric fields and magnetic properties down to the single atom level. The precisely defined interfaces will enable quantitative comparison with *ab initio* theory and a better understanding of the underlying physical principles.

Financial support from Grants No. SFB 668-B4 and No. GrK 1286 of the Deutsche Forschungsgemeinschaft and from the ERC Advanced Grant "FURORE" is gratefully acknowledged.

*asonntag@physnet.uni-hamburg.de

[1] H. Ohno, D. Chiba, F. Matsukura, T. Omiya, E. Abe, T. Dietl, Y. Ohno, and K. Ohtani, Nature (London) **408**, 944 (2000).
[2] D. Chiba, M. Yamanouchi, F. Matsukura, and H. Ohno, Science **301**, 943 (2003).
[3] W. Eerenstein, N. D. Mathur, and J. F. Scott, Nature (London) **442**, 759 (2006).
[4] M. Weisheit, S. Fähler, A. Marty, Y. Souche, C. Poinsignon, and D. Givord, Science **315**, 349 (2007).
[5] D. Chiba, M. Sawicki, Y. Nishitani, Y. Nakatani, F. Matsukura, and H. Ohno, Nature (London) **455**, 515 (2008).

[6] Y.-H. Chu, L. W. Martin, M. B. Holcomb, M. Gajek, S.-J. Han, Q. He, N. Balke, C.-H. Yang, D. Lee, W. Hu *et al.*, Nat. Mater. **7**, 478 (2008).
[7] T. Maruyama, Y. Shiota, T. Nozaki, K. Ohta, N. Toda, M. Mizuguchi, A. A. Tulapurkar, T. Shinjo, M. Shiraishi, S. Mizukami *et al.*, Nat. Nanotechnol. **4**, 158 (2009).
[8] L. Gerhard, T. K. Yamada, T. Balashov, A. F. Takács, R. J. H. Wesselink, M. Däne, M. Fechner, S. Ostanin, A. Ernst, I. Mertig *et al.*, Nat. Nanotechnol. **5**, 792 (2010).
[9] H. K. D. Kim, L. T. Schelhas, S. Keller, J. L. Hockel, S. H. Tolbert, and G. P. Carman, Nano Lett. **13**, 884 (2013).
[10] K. Nakamura, R. Shimabukuro, Y. Fujiwara, T. Akiyama, T. Ito, and A. J. Freeman, Phys. Rev. Lett. **102**, 187201 (2009).
[11] M. Tsujikawa and T. Oda, Phys. Rev. Lett. **102**, 247203 (2009).
[12] C.-G. Duan, J. P. Velev, R. F. Sabirianov, Z. Zhu, J. Chu, S. S. Jaswal, and E. Y. Tsymbal, Phys. Rev. Lett. **101**, 137201 (2008).
[13] M. Endo, S. Kanai, S. Ikeda, F. Matsukura, and H. Ohno, Appl. Phys. Lett. **96**, 212503 (2010).
[14] T. Nozaki, Y. Shiota, M. Shiraishi, T. Shinjo, and Y. Suzuki, Appl. Phys. Lett. **96**, 022506 (2010).
[15] M. Bode, S. Krause, L. Berbil-Bautista, S. Heinze, and R. Wiesendanger, Surf. Sci. **601**, 3308 (2007).
[16] U. Gradmann, G. Liu, H. J. Elmers, and M. Przybylski, Hyperfine Interact. **57**, 1845 (1990).
[17] H. J. Elmers, J. Hauschild, H. Höche, U. Gradmann, H. Bethge, D. Heuer, and U. Köhler, Phys. Rev. Lett. **73**, 898 (1994).
[18] M. Bode, O. Pietzsch, A. Kubetzka, and R. Wiesendanger, Phys. Rev. Lett. **92**, 067201 (2004).
[19] M. L. Néel, Ann. Géophys. **5**, 99 (1949).
[20] W. F. Brown, Phys. Rev. **130**, 1677 (1963).
[21] W. Wernsdorfer, E. B. Orozco, K. Hasselbach, A. Benoit, B. Barbara, N. Demoncy, A. Loiseau, H. Pascard, and D. Mailly, Phys. Rev. Lett. **78**, 1791 (1997).
[22] S. Krause, G. Herzog, T. Stapelfeldt, L. Berbil-Bautista, M. Bode, E. Y. Vedmedenko, and R. Wiesendanger, Phys. Rev. Lett. **103**, 127202 (2009).
[23] A. Schlenhoff, S. Krause, A. Sonntag, and R. Wiesendanger, Phys. Rev. Lett. **109**, 097602 (2012).
[24] S. Krause, G. Herzog, A. Schlenhoff, A. Sonntag, and R. Wiesendanger, Phys. Rev. Lett. **107**, 186601 (2011).
[25] S. Krause, L. Berbil-Bautista, G. Herzog, M. Bode, and R. Wiesendanger, Science **317**, 1537 (2007).
[26] See Supplemental Material at http://link.aps.org/supplemental/10.1103/PhysRevLett.112.017204 for the determination of the electric field strength.
[27] L. Xu and S. Zhang, J. Appl. Phys. **111**, 07C501 (2012).
[28] R. Shimabukuro, K. Nakamura, T. Akiyama, and T. Ito, Physica (Amsterdam) **42E**, 1014 (2010).
[29] A. Schlenhoff, S. Krause, G. Herzog, and R. Wiesendanger, Appl. Phys. Lett. **97**, 083104 (2010).
[30] K. Nakamura, T. Akiyama, T. Ito, M. Weinert, and A. J. Freeman, Phys. Rev. B **81**, 220409 (2010).